Optik 124 (2013) 3187–3193

Contents lists available at SciVerse ScienceDirect

Optik

journal homepage: www.elsevier.de/ijleo

A non-circular iris localization algorithm using image projection function and gray level statistics

Farmanullah Jan*, Imran Usman, Shahrukh Agha

Department of Electrical Engineering, COMSATS Institute of Information Technology, Park Road, Chak Shahzad, 44000 Islamabad, Pakistan

ARTICLE INFO

Article history:
Received 11 April 2012
Accepted 23 September 2012

Keywords:
Iris localization
Histogram
Biometrics
Iris recognition
Active contours

ABSTRACT

Iris recognition technology identifies an individual from its iris texture with great precision. A typical iris recognition system comprises eye image acquisition, iris segmentation, feature extraction, and matching. However, the system precision greatly depends on accurate iris localization in the segmentation module. In this paper, we propose a reliable iris localization algorithm. First, we locate a coarse eye location in an eye image using integral projection function (IPF). Next, we localize the pupillary boundary in a sub image using a reliable technique based on the histogram-bisection, image statistics, eccentricity, and object geometry. After that, we localize the limbic boundary using a robust scheme based on the radial gradients and an error distance transform. Finally, we regularize the actual iris boundaries using active contours. The proposed algorithm is tested on public iris databases: MMU V1.0, CASIA-IrisV1, and the CASIA-IrisV3-Lamp. Experimental results demonstrate superiority of the proposed algorithm over some of the contemporary techniques.

1. Introduction

In recent years, information technology has undergone through enormous developmental phases that caused maturity in both the software and hardware platforms, for instance, cell phones, auto teller machines, and the Google-map are to name a few. Despite of these advances, the life and assets of an individual are not safe. Every day, we hear about the criminal activities, such as cybercrimes, bank frauds, hacking of passwords and personal identification numbers, and so on. Most often, it is found that such happenings occur because of loopholes present in the traditional security systems [1–3], which use the knowledge and tokens based techniques (e.g., keys, identity cards, passwords, etc.), which could be shared and/or hacked. Due to these imperfections, traditional security systems are now being replaced by the biometric technology [1–3].

Biometric technology uses the physiological and/or physical traits to authenticate identity of an individual [2,4,5]. It includes retina, iris, signature, ear, face, smell, palm, fingerprint, gait, DNA, and among the others [2,4–7]. Traits, such as fingerprint, signature, voice, and face, have long been in use for the human identification and verification. However, these traits may change with the subject aging effects and could be duplicated artificially as well. On other hand, iris texture could not be copied and/or changed by any artificially means, except its intentional surgery [4]. In human eye, iris is an annulus located between the pupil and sclera, which is protected by the cornea. In addition to its stable, unique, and non-invasive properties, it has quite complex structure comprising ridges, corona, furrows, crypts, freckles, and the arching ligaments [4,5]. Literature reveals that iris structure remains stable over the entire life period of a subject, except some negligible changes in the early life stages [4,5]. Iris technology has great potential for its applications; for example, citizen registration department, border-crossing control, sales points, health and care department, travel and immigration agencies, and so on.

A typical iris recognition system includes image acquisition, iris segmentation, feature extraction, and matching and recognition [2]. However, among these modules, iris segmentation plays a vital role in the overall system accuracy, because all the subsequent modules follow its results. It localizes the iris inner (pupillary boundary) and outer (limbic boundary) boundaries at the pupil and sclera, respectively; and detects and excludes any other noise, such as eyelids, eyelashes, and/or specular reflections [3,4]. This study focuses on accurate localization of pupillary and limbic boundaries only (as in [3,8]). In [4], Daugman localized these boundaries with a circle approximation using an Integro-differential operator (IDO). Similarly, Wildes [5] used a combination of circular Hough transform (CHT) and the gradient edge-map to localize iris. Following that, numerous researchers proposed different segmentation techniques [2], which are based on these pioneered ideas [4,5]. However, iris localization techniques [2,3,8] that use CHT and/or IDO consume relatively more time compared to the methods based on the histogram and thresholding based techniques [3].

* Corresponding author.
E-mail address: farmanullahs123@yahoo.com (F. Jan).

0030-4026/$ – see front matter © 2012 Elsevier GmbH. All rights reserved.
http://dx.doi.org/10.1016/j.ijleo.2012.09.018

Khan et al. [3] proposed an iterative strategy based on the histogram and eccentricity to localize pupillary boundary in a binary image, which has some flaws; for example, they first convert the eye image to a binary image and, then check eccentricity by considering the whole image as a binary object. However, in case, if an eye image contains other low intensity regions (e.g., eyebrows, eyelashes, and hair), then the resultant binary image may contain multiple objects and this method will face its outage. Similarly, Ibrahim et al. [8] used standard deviations of the pixels' coordinates of a binary object to localize pupil. However, they also did not propose any method to handle with multiple objects. Thus, to resolve this issue, we propose an iris localization technique that comprises an adaptive threshold, eccentricity, area, and binary object geometry. Moreover, authors in [3,8] localized limbic boundary with a circle approximation. They used radial gradients in horizontal direction to estimate radius of the iris circle. However, to some extent, this technique is quite effective, but they fail to extract the precise center for iris circle. To estimate center coordinates, they compute *y*-coordinate from the absolute distances of the left and the right boundary points having maximum gradients. Next, they assign *x*-coordinate of the pupil circle to *x*-coordinate of the iris circle. Due to this assignment, the iris circle may be either pushed up or down along the *y*-axis. It may cause significant number of iris pixels to be left outside and vice versa. Thus, to resolve this problem too, we propose an effective scheme that does not even need an iris center: first, we extract radius for the circular limbic boundary using radial gradients in two secure regions. Next, we mark circular limbic boundary with its center at the pupil center. Finally, we apply active contours to regularize the pupillary and limbic boundaries. This regularization process effectively compensates for any offset in the pupil and iris' centers.

Rest of the paper is structured as follows. Section 2 details different modules of the proposed technique whereas Section 3 presents experimental results and discussion. Limitations of the proposed technique are explained in Section 4 and finally, this study is concluded in Section 5.

2. Proposed iris localization method

The proposed technique includes the following modules: pupillary boundary localization (PBL), limbic boundary localization (LBL), and iris boundaries regularization (IBR).

2.1. Pupillary boundary localization

As indicated in Fig. 2(a), generally, the input eye image contains regions, such as skin, sclera, iris, pupil, eyelids, eyelashes, specular reflections, and eyebrows. However, among these regions the pupil, eyelashes, eyebrows, and hair may have relatively the same gray level intensities, which fortunately, differ from each other by their respective geometry, for instance, eyelashes, eyebrows, and the hair may have large length compared to width. On other hand, a pupil region is compact; therefore, s aspect ratio (i.e., length to width ratio) would always be within a specific threshold. Due to these arguments, we propose a robust scheme to localize pupillary boundary with circle approximation using eccentricity, area, geometry, and the image gray level statistics. Fig. 1 shows flow diagram of pupil localization scheme, which includes four stages that are elaborated in the following text.

2.1.1. Stage-I

This stage is consisted of the following two steps:

1. Literature reveals that illuminator of the image acquisition device causes specular reflections in iris images [4]. As specular reflections encumber most of the iris segmentation techniques [2]; therefore, we suppress them prior to start the iris localization process. To begin with, first complement the gray level input eye image $I_g(x,y)$ as $\hat{I}_g(x,y) = 255 - I_g(x,y)$. Next, use a 4-connectivity procedure [9] to detect and invert gray level values of holes in $\hat{I}_g(x,y)$; a region of dark pixels surrounded by lighter pixels is called a hole (see Fig. 2(b)). After that, complement $\hat{I}_g(x,y)$ and pass the resultant image through a median filter (windows size [12 12]) to get the preprocessed eye image $I_p(x,y)$. Finally, stretch contrast of $I_p(x,y)$ to the full gray scale range 0–255 [3,9], see Fig. 2(d).
2. Use the vertical ($M_v(x)$) and horizontal ($M_h(y)$) Integral projection functions [1] to locate a Seed-pixel (S_x,S_y) in the iris/pupil region. Where S_x and S_y represent the *x*- and *y*-coordinates of Seed-pixel, respectively.

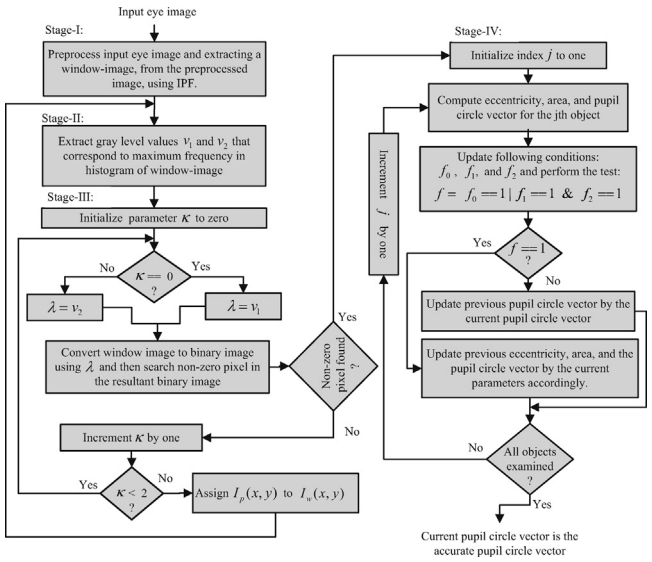

Fig. 1. Flow chart of module PBL.

$$M_v(x) = \frac{1}{n}\sum_{i=1}^{n} I(x, y_i), \quad x = 1, 2, 3, \ldots, m, \tag{1}$$

$$M_h(y) = \frac{1}{m}\sum_{i=1}^{m} I(x_i, y), \quad y = 1, 2, 3, \ldots, n, \tag{2}$$

where m and n represent the number of rows and columns of $I_p(x,y)$, respectively. After computing M_v and M_h, extract (S_x,S_y)-coordinates as $S_x[x_o \in \{x = 1, 2, 3, \ldots, m\}$ such that $M_v(x)$ is maximum at $x = x_o]$, $S_y[y_o \in \{y = 1, 2, 3, \ldots, n\}$ such that $M_h(y)$ is maximum at $y = y_o]$.

Fig. 3(a) and (b) shows the vertical and horizontal integral projection functions, respectively, whereas Fig. 3(c) shows a Window-image $I_w(x,y)$ centered at (S_x,S_y); its each side is set to 60% of width of $I_p(x,y)$. From now on, we use $I_w(x,y)$ as the input image for further processing unless stated otherwise.

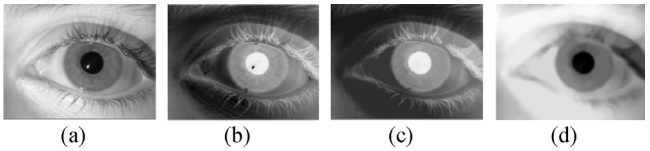

Fig. 2. (a) Gray level input eye image $I_g(x,y)$. (b) Complemented image $\hat{I}_g(x,y)$; black dot in pupil region represents hole. (c) $\hat{I}_g(x,y)$ with holes suppressed. (d) Preprocessed image $I_p(x,y)$.